Inorg. Chem. **2007**, *46*, 11224–11234

Determination of the Intrinsic Affinities of Multiple Site-Specific Mg^{2+} Ions Coordinated to Domain 6 of a Group II Intron Ribozyme†

Michèle C. Erat and Roland K. O. Sigel*

Institute of Inorganic Chemistry, University of Zürich, Winterthurerstrasse 190, CH-8057 Zürich, Switzerland

Received August 16, 2007

Group II introns are large metallo-ribozymes that use divalent metal ions in folding and catalysis. The 3′-terminal domain 6 (D6) contains a conserved adenosine whose 2′-OH group acts as the nucleophile in the first splicing step. In the hierarchy of folding, D6 binds last into the active site. In order to investigate and understand the folding process to the catalytically active intron structure, it is important to know the individual binding affinities of Mg^{2+} ions to D6. We recently studied the solution structure of a 27 nucleotide long D6 (D6-27) from the mitochondrial yeast group II intron Sc.ai5γ, also identifying five Mg^{2+} binding sites including the one at the 5′-terminal phosphate residues. Mg^{2+} coordination to the 5′-terminal di- and triphosphate groups is strongest (e.g., log $K_{A,TP} = 4.55 \pm 0.10$) and is evaluated here in detail for the first time. The other four binding sites within D6-27 are filled simultaneously (e.g., log $K_{A,BR} = 2.38 \pm 0.06$) and thus compete for the free Mg^{2+} ions in solution, having a distinct influence on the individual affinities of the various sites. For the first time, we take this competition into account to obtain the intrinsic binding constants, describing a method that is generally applicable. Our data illustrates that any RNA molecule undergoing tertiary contacts to a second RNA molecule first needs to be loaded evenly and specifically with metal ions to compensate for the repulsion between the negatively charged RNA molecules.

Introduction

Group II introns are highly structured, autocatalytic RNA molecules of 600−2500 nucleotides in length.[1] They occur in organellar genes in plants, algae, fungi, and yeast, as well as in some bacterial genomes. Group II introns catalyze their own removal from the pre-mRNA in a mechanism that is at first sight highly similar to the one performed by the eukaryotic multicomponent splicing machinery, the so-called spliceosome. However, in contrast to the spliceosome, group II introns are able to splice without the aid of external protein factors and are thus true ribozymes.

Group II introns have a conserved secondary structure consisting of six individual domains that project from a central wheel (Figure 1a). These domains are structurally distinct and have individual functions in folding and catalysis.[1,2] Domain 6 (D6) thereby actively takes part in splicing as this domain contains a highly conserved bulged adenosine whose 2′-OH group is the nucleophile in the first step of splicing.[3−6] We have recently solved the NMR solution structure of a minimal but active branch D6 from the yeast mitochondrial group II intron Sc.ai5γ (Figure 1).[7] This so-called D6-27 construct retains all important branching determinants that lie within the branch domain itself[8] and has been shown to actively trans-splice in vitro.[7] In this group II intron D6, the branch adenosine is stacked within the helix, which is in contrast to the branch-point conformation in the spliceosome.[9] Interestingly, the addition of millimolar concentrations of Mg^{2+} leads to a further increase in stacking

* To whom correspondence should be addressed. E-mail: roland.sigel@aci.uzh.ch. Phone: ++41-44-635 4652. Fax: ++41-44-635 6802.

† With the best wishes of the authors to Professor H. Sigel, University of Basel, on the occasion of his 70th birthday.

(1) Lehmann, K.; Schmidt, U. *Crit. Rev. Biochem. Mol. Biol.* **2003**, *38*, 249−303.
(2) Qin, P. Z.; Pyle, A. M. *Curr. Opin. Struct. Biol.* **1998**, *8*, 301−308.
(3) Michel, F.; Ferat, J. L. *Annu. Rev. Biochem.* **1995**, *64*, 435−461.
(4) Pyle, A. M. Catalytic reaction mechanisms and structural features of group II intron ribozymes. In *Nucleic Acids and Molecular Biology*; Eckstein, F., Lilley, D. M. J., Eds.; Springer-Verlag: New York, 1996; Vol. 10, pp 75−107.
(5) Liu, Q.; Green, J. B.; Khodadadi, A.; Haeberli, P.; Beigelman, L.; Pyle, A. M. *J. Mol. Biol.* **1997**, *267*, 163−171.
(6) Abramovitz, D. L.; Friedman, R. A.; Pyle, A. M. *Science* **1996**, *271*, 1410−1413.
(7) Erat, M. C.; Zerbe, O.; Fox, T.; Sigel, R. K. O. *ChemBioChem* **2007**, *8*, 306−314.
(8) Chu, V. T.; Liu, Q.; Podar, M.; Perlman, P. S.; Pyle, A. M. *RNA* **1998**, *4*, 1186−1202.
(9) Newby, M. I.; Greenbaum, N. L. *Biophys. J.* **2002**, *82*, 131a.

10.1021/ic701627t CCC: $37.00
Published on Web 11/29/2007

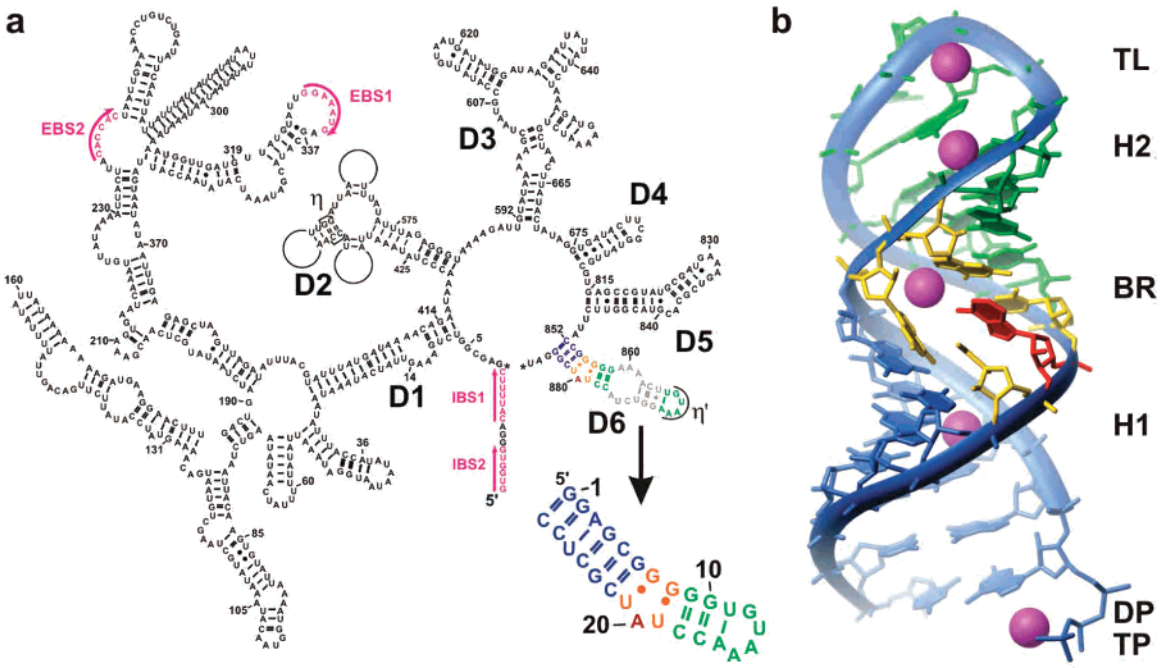

Figure 1. Group II intron Sc.ai5γ from yeast mitochondria together with the NMR structure of a shortened branch D6: (a) Secondary structure of Sc.ai5γ and of the shortened NMR construct D6-27 with the corresponding nucleotides colored accordingly. The tetraloop−tetraloop receptor interaction $\eta-\eta'$ between D2 and D6 is indicated. The exon binding sites (EBS1 and EBS2) and the corresponding intron binding sites (IBS1 and IBS2) are colored in pink. (b) NMR solution structure of D6-27 with five Mg^{2+} ions (magenta spheres) modeled by hand into the presumed binding sites and labeled as explained in the text. The structure has been drawn with *MOLMOL*[18] and is based on the PDB structure coordinates 2AHT.[7]

interactions of the branch adenosine and its neighboring bases, as was shown by fluorescence measurements.[7]

The folding of group II introns follows a distinct pathway, whereby the largest D1 folds first to provide the scaffold for the other domains.[10] Hence, D5 and D6 dock into the prefolded D1, whereby D5 drags the branch D6 into the single active site.[11,12] The Mg^{2+} requirement for the folding of the Sc.ai5γ intron in vitro differs for the individual folding steps: Whereas the central region of D1, constituting the nucleation region for folding only, requires about 5 mM $MgCl_2$, the final fold of D1 and the assembly of the other domains requires about 40 mM Mg^{2+}.[13,14] In the active ribozyme structure, the metal ions occupy distinct sites, several of them being part of the catalytic core.[15−17] In order to understand the single steps of folding and the formation of the metal ion binding pockets, it is a prerequisite to know the metal ion binding sites within the isolated domains as well as their individual loading factor with Mg^{2+} ions.

Several metal ion binding sites have previously been detected in D6: The crystal structure of a permuted D56 construct (D56 = RNA construct containing domains 5 and 6) showed a cobalt(III)hexammine near the branch nucleotides,[19] and Tb^{3+} cleavage experiments have revealed metal ion binding in the minor groove of the branch adenosine within the full-length group II intron.[15,20] In addition, our recent NMR studies on the shortened D6-27 construct[7] have revealed one Mg^{2+} ion in the major groove of the branch adenosine and the two adjacent GU wobble pairs. The binding of this Mg^{2+} ion leads to increased stacking of the branch adenosine within the helix of D6-27, as was recently shown by the steady decrease in fluorescence emission of a 2-aminopurine inserted at the branch-site of D6-27.[7] Three further Mg^{2+} coordination sites within the D6-27 hairpin were proposed based on these NMR experiments, i.e., in the tetraloop, and one each in the helical regions below and above the branch adenosine (Figure 1b).[7] At last, actually the strongest binding site is found at the 5′-terminal triphosphate group, which is a reminder of every transcription, but nevertheless still needs to be taken into account when calculating affinity constants of uncapped RNAs, as resulting from in vitro transcription by T7 polymerase. Interestingly, uncapped 5′-triphosphates have recently been implicated as the molecular signal for the detection of viral infections.[21,22]

To pinpoint the Mg^{2+} ion binding sites within D6-27 and to determine their intrinsic affinities in detail, we have now performed paramagnetic line-broadening experiments with Mn^{2+} as well as extensive titration studies with Mg^{2+} by

(10) Qin, P. Z.; Pyle, A. M. *Biochemistry* **1997**, *36*, 4718−4730.
(11) Chu, V. T.; Adamidi, C.; Liu, Q.; Perlman, P. S.; Pyle, A. M. *EMBO J.* **2001**, *20*, 6866−6876.
(12) de Lencastre, A.; Hamill, S.; Pyle, A. M. *Nat. Struct. Mol. Biol.* **2005**, *12*, 626−627.
(13) Sigel, R. K. O. *Eur. J. Inorg. Chem.* **2005**, *12*, 2281−2292.
(14) Waldsich, C.; Pyle, A. M. *Nat. Struct. Mol. Biol.* **2007**, *14*, 37−44.
(15) Sigel, R. K. O.; Vaidya, A.; Pyle, A. M. *Nat. Struct. Biol.* **2000**, *7*, 1111−1116.
(16) Gordon, P. M.; Piccirilli, J. A. *Nat. Struct. Biol.* **2001**, *8*, 893−898.
(17) Gordon, P. M.; Sontheimer, E. J.; Piccirilli, J. A. *Biochemistry* **2000**, *39*, 12939−12952.
(18) Koradi, R.; Billeter, M.; Wüthrich, K. *J. Mol. Graphics* **1996**, *14*, 29−32 and 51−55.
(19) Zhang, L.; Doudna, J. A. *Science* **2002**, *295*, 2084−2088.
(20) Sigel, R. K. O.; Pyle, A. M. *Met. Ions Biol. Syst.* **2003**, *40*, 477−512.
(21) Hornung, V.; Ellegast, J.; Kim, S.; Brzozka, K.; Jung, A.; Kato, H.; Poeck, H.; Akira, S.; Conzelmann, K. K.; Schlee, M.; Endres, S.; Hartmann, G. *Science* **2006**, *314*, 994−997.
(22) Pichlmair, A.; Schulz, O.; Tan, C. P.; Naslund, T. I.; Liljestrom, P.; Weber, F.; Sousa, C. R. E. *Science* **2006**, *314*, 997−1001.

Table 1. Log $K_{A,est}$ Values for Mg^{2+} Binding to D6-27: Individual log $K_{A,est}$ Values Obtained from the Change in Chemical Shifts of All Aromatic and H1′ Protons in D6-27 after the First Round of Calculation in Which the Mg^{2+} Concentration Corresponds to the Total Amount of Mg^{2+} Added at Each Titration Point.[a] The Nucleotides Belonging to the Five Individual Binding Sites Are Shaded by Alternative Grey Scales (from left to right: 5′-end (DP/TP); helix 1 (H1); branch region (BR); helix 2 (H2); tetraloop (TL))

	DP/TP			H1			BR				H2		TL	
residue	G1	G2	A3	G4	C5	G6	G7		G8	G9	G10	U11	G12	U13
H1′	2.38 ± 0.22[b]	2.31 ± 0.26[b]	1.66 ± 0.18	n.d.[c]	n.d.[c]	n.d.[c]	1.71 ± 0.07		n.d.[c]	n.d.[c]	n.d.[c]	1.71 ± 0.17	n.d.[d]	1.91 ± 0.11
H2/H5	–	–	n.d.[c]	–	1.82 ±0.25	–	–		–	–	–	2.04 ± 0.12	–	1.58 ± 0.14
H6/H8	n.d.[b,c]	n.d.[b]	n.d.[c]	2.23 ± 0.14	n.d.[c]	n.d.[c]	1.61 ± 0.15		2.07 ± 0.07	1.93 ± 0.25	2.03 ± 0.14	1.72 ± 0.16	1.89 ± 0.29	n.d.[c]
residue	C27	C26	U25	C24	G23	C22	U21	A20	U19	C18	C17	A16	A15	A14
H1′	1.78 ± 0.15	n.d.[c]	1.49 ± 0.43	1.88 ± 0.13	1.90 ± 0.19	1.74 ± 0.11	2.06 ± 0.09	2.23 ± 0.08	2.07 ± 0.15	n.d.[c]	2.38 ± 0.22	n.d.[c]	1.80 ± 0.09	2.06 ± 0.14
H2/H5	n.d.[c]	n.d.[c]	1.85 ± 0.22	n.d.[c]	–	2.11 ± 0.09	2.23 ± 0.07	1.98 ± 0.11	n.d.[c]	n.d.[c]	1.81 ± 0.21	n.d.[c]	2.05 ± 0.10	1.42 ± 0.26
H6/H8	n.d.[c]	n.d.[c]	2.19 ± 0.11	n.d.[d]	n.d.[c]	n.d.[c]	2.11 ± 0.09	2.25 ± 0.09	1.63 ± 0.16	n.d.[c]	1.74 ± 0.11	n.d.[d]	1.88 ± 0.15	n.d.[c]

[a] The chemical shift changes were obtained from [^{1}H,^{1}H]-NOESY spectra in D_2O (0.85 mM D6-27 RNA, pD 6.7, 100 mM KCl, 10 μM EDTA, 30 °C). The log K_A values were calculated with a Levenberg−Marquardt nonlinear least-squares regression for a single binding isotherm (eq 4). The five individual binding sites were identified by Mg^{2+} titrations as well as by Mg^{2+} and Mn^{2+} line-broadening data. All error limits given correspond to 1 standard deviation (1σ). [b] Values are given for Mg^{2+} binding to D6-27 with a 5′-terminal diphosphate. With a 5′-terminal triphosphate group, log $K_A = 3.15 \pm 0.11$ ($G1_{TP}H8$). [c] n.d., not determined, because chemical shift changes were too small. [d] n.d., not determined, as peaks are getting too broad with higher Mg^{2+} concentrations.

NMR. By evaluating for the first time the changes in chemical shifts of both base and sugar protons in the branch domain, determined the affinity constants for Mg^{2+} binding to five distinct sites in D6-27 (Figure 1b). As these preliminary affinities only vary by a factor of about 10, the five coordination sites within this hairpin must fill up in parallel. As a consequence, at every step of the titration, a certain amount of the total Mg^{2+} present is not available to bind to a given site. To the best of our knowledge, this effect has never been taken into account when calculating the affinity constants of metal ion binding sites in RNA. Hence, we describe here a new iterative correction procedure that allows us to determine the intrinsic Mg^{2+} affinity at each site by taking the binding to the other sites into account. This procedure is generally applicable to any RNA molecule that harbors several specific coordination sites for metal ions.

Experimental Section

Materials. DNA oligonucleotides were purchased from Microsynth, Balgach (Switzerland), and the nucleotide 5′-triphosphates came from GE Healthcare (formerly Amersham Biosciences Europe GmbH, Otelfingen (Switzerland)), except for UTP, which was obtained from Sigma-Aldrich-Fluka, Buchs (Switzerland). T7 polymerase used for in vitro transcription was homemade.[23,24] The electroelution apparatus Biotrap was from Schleicher & Schuell, Dassel (Germany). For desalting, Centricon centrifugal filter devices (3000 MWCO) from Amicon were used. $MgCl_2$ for the metal ion titration was obtained as 1 M ultrapure solution in H_2O from Fluka. The exact concentration of the $MgCl_2$ and $MnCl_2$ stock solution in 99.999% D_2O (Sigma-Aldrich) was determined by potentiometric pH titration employing EDTA. All chemicals used were at least puriss p.a. and purchased from either Fluka-Sigma-Aldrich or Brunschwig Chemie, Amsterdam (The Netherlands).

NMR Sample Preparation: D6-27 (5′-GGAGCGGGGGU-GUAAACCUAUCGCUCC) was synthesized by in vitro transcription with T7 polymerase and purified as described.[7] After desalting and lyophilization, the sample was dissolved in 220 μL of D_2O (100 mM KCl, 10 μM EDTA, pD 6.7). To measure the pD value, 0.4 log units were added to the pH meter reading.[25,26] The RNA concentration was determined with a Varian Cary 500 Scan UV−vis−NIR spectrophotometer, using an extinction coefficient at 260 nm (ϵ_{260}) of 296.3 mM^{-1} cm^{-1} for D6-27. All samples were lyophilized and resuspended in either 90% H_2O/10% D_2O or 99.999% D_2O prior to the acquisition of NMR spectra.

NMR Spectroscopy. NMR spectra were recorded on a Bruker AV700 MHz spectrometer equipped with a CP-TXI *z*-axis pulsed-field gradient cryoprobe. NMR spectra were processed with *XWINNMR* and *TOPSPIN* 3.1 (Bruker) and analyzed using *Sparky* (http://www.cgl.ucsf.edu/home/sparky/).

Mn^{2+} and Mg^{2+} Line-Broadening Experiments. Mn^{2+} binding was monitored by titrating a sample of 1.1 mM D6-27 (99.999% D_2O, $I = 0.1$ M (KCl), 10 μM EDTA, pD = 6.7), in steps of 0, 15, 30, 45, 60, 90, and 120 μM $MnCl_2$ (i.e., $[Mn^{2+}]_{tot} = 0$, 5, 20, 35, 50, 80, and 110 μM) and acquisition of [^{1}H,^{1}H]-NOESY (NOESY = Nuclear Overhauser Spectroscopy) spectra each with 64 scans and 1024 experiments in F2 as well as 256 experiments in F1 at 303 K. Mg^{2+} line broadening was monitored by a [^{1}H,^{1}H]-NOESY series with 0.85 mM D6-27 (99.999% D_2O, $I = 0.1$ M (KCl), 10 μM EDTA, pD = 6.74), and steps of 0, 1, 2, 3, 4, 5, 6, 7, 8, 10, and 12 mM $MgCl_2$.

Mg^{2+} Titrations and Calculation of Stability Constants. The concentration of D6-27 RNA in the titration experiments was 0.85 mM. Integration of NOESY peaks associated with the 5′-end of the hairpin yielded a 1:2 ratio of molecules with either a 5′-terminal triphosphate chain or a diphosphate. Thus, RNA concentrations of 0.28 and 0.57 mM, respectively, were used for calculating the affinity constants of Mg^{2+} to the 5′-termini. Mg^{2+} binding to D6-27 was monitored by observing the changes in chemical shifts of the aromatic and sugar protons in [^{1}H,^{1}H]-NOESY spectra acquired in the presence of 0, 1, 2, 3, 4, 5, 6, 7, 8, 10, and 12 mM $MgCl_2$ (99.999% D_2O, $I = 0.1$ M (KCl), 10 μM EDTA, pD = 6.7). The chemical shift of the protons (aromatic as well as H1′) showing the largest changes were plotted against the Mg^{2+} concentration and fitted to a single binding isoterm using a Levenberg−Marquardt nonlinear least-squares regression.[27,28] From these fits, the first estimates for millimolar affinity constants $K_{A,est}$ were calculated by using the total amount of Mg^{2+} present in solution (Table 1). The $K_{A,est}$ values were grouped according to five individual binding

(23) Davanloo, P.; Rosenberg, A. H.; Dunn, J. J.; Studier, F. W. *Proc. Natl. Acad. Sci. U.S.A.* **1984**, *A81*, 2035−2039.
(24) Gallo, S.; Furler, M.; Sigel, R. K. O. *Chimia* **2005**, *59*, 812−816.
(25) Lumry, R.; Smith, E. L.; Glantz, R. R. *J. Am. Chem. Soc.* **1951**, *73*, 4330−4340.
(26) Glasoe, P. K.; Long, F. A. *J. Phys. Chem.* **1960**, *64*, 188−190.

Table 2. Affinity Values log K_A for Mg^{2+} Binding to D6-27 in D_2O. Listed Are the Averaged log $K_{A,av}$ Values (1σ) at the Five High-Affinity Binding Sites, Obtained from the Change in Chemical Shifts of All Aromatic and H1′ Protons after Various Rounds of Iterative Corrections for the Mg^{2+} Concentration That is Available at a Certain Site. For the 5′-end, Values Are Given for the Di- and Triphosphate Case (5′-end GDP and 5′-end GTP)[a]

binding site	log $K_{A,av1}$	log $K_{A,av2}$	log $K_{A,av3}$	log $K_{A,av4}$	log $K_{A,av5}$	log $K_{A,fin}$[b]	$\Delta_{fin-av1}$[c]
5′-end GDP (DP)[d]	2.35 ± 0.04	2.56 ± 0.04	2.67 ± 0.04	2.74 ± 0.04	2.78 ± 0.05	2.83 ± 0.03	0.48 ± 0.05
5′-end GTP (TP)[d]	3.15 ± 0.11	3.34 ± 0.11	3.49 ± 0.11	3.61 ± 0.11	3.69 ± 0.11	4.04 ± 0.10	0.89 ± 0.15
helix 1 (H1)	1.91 ± 0.09	2.14 ± 0.08	2.23 ± 0.07	2.29 ± 0.07	2.31 ± 0.07	2.33 ± 0.03	0.42 ± 0.09
branch site (BR)	1.88 ± 0.10	2.12 ± 0.09	2.26 ± 0.08	2.33 ± 0.07	2.34 ± 0.08	2.38 ± 0.06	0.50 ± 0.12
helix 2 (H2)	1.80 ± 0.14	2.06 ± 0.11	2.16 ± 0.11	2.21 ± 0.12	2.24 ± 0.12	2.25 ± 0.03	0.45 ± 0.14
tetraloop (TL)	1.76 ± 0.09	2.00 ± 0.08	2.07 ± 0.08	2.11 ± 0.08	2.14 ± 0.08	2.14 ± 0.03	0.38 ± 0.09

[a] The chemical shift changes were obtained from 2D [^{1}H,^{1}H]-NOESY spectra of a 0.85 mM D6-27 RNA at pD 6.7 in 100 mM KCl at 30 °C. All error limits given for the log $K_{A,av}$ values correspond to 1 standard deviation (1σ). [b] The maximal log $K_{A,fin}$ values correspond to the limiting value of an asymptotic fit obtained from plotting log $K_{A,av}$ after each round of correction versus the number of the iteration round (Figure 5). The errors of these fits were small throughout and thus multiplied by 3 to obtain values we consider as reasonable error limits. The error limit for log $K_{A,TP}$ is an estimate because the result from the fitting calculation (±0.01) is too small considering the extent of extrapolation and the fact that this site is saturated to a large part already at 1 mM Mg^{2+} (Table 3). [c] Difference in log K_A between the original values obtained from fits of the chemical shift change versus the titrated [Mg^{2+}] and the maximal log $K_{A,fin}$ of the asymptotic fit (see footnote *b*). [d]The values given in this table are apparent stability constants valid for pD 6.7. The actual affinity constants corrected for the competition with the proton are log $K_{A,TP} = 4.55 \pm 0.10$ for the triphosphate 5′-end and log $K_{A,DP} = 3.26 \pm 0.03$ for the diphosphate 5′-end; see text.

sites, based on their agreement within the error limits and the line-broadening data (see also Results and Discussion section and Supporting Information Table S1). Next, for each individual site an average $K_{A,av}$ value was calculated (see Results and Table 2).

The averaged $K_{A,av1}$ values of the first estimates were used to calculate the amount of Mg^{2+} bound to each binding site and thus to determine the actual free Mg^{2+} concentration in the following way: For each internal binding site "*i*" in D6-27, the equilibrium

$$RNA_i + Mg^{2+} \rightleftarrows RNA_i{\cdot}Mg^{2+} \tag{1a}$$

and the definition of its affinity constant

$$K_{A_i} = \frac{[RNA_i{\cdot}Mg^{2+}]}{[Mg^{2+}]_i[RNA_i]} \tag{1b}$$

holds, together with eqs 2 and 3,

$$[Mg^{2+}]_{tot} = [RNA_i{\cdot}Mg^{2+}]_i + [Mg^{2+}]_{tot-i} \tag{2}$$

and

$$[RNA_i]_{tot} = [RNA_i{\cdot}Mg^{2+}]_i + [RNA]_{tot-i} \tag{3}$$

$[Mg^{2+}]_{tot}$ and $[RNA_i]_{tot}$ correspond to the total concentration of Mg^{2+} or RNA available for each individual binding site, respectively, $[RNA_i{\cdot}Mg^{2+}]$ corresponds to the concentration of the complexed species, and $[Mg^{2+}]_{tot-i}$ and $[RNA_i]_{tot-i}$ correspond to the concentration of the free species present in solution. The change in chemical shift in such a 1:1 binding equilibrium of eq 1a can be described by eq 4

$$\Delta\delta_{obs} = \Delta\delta_{RNA_i} + (\Delta\delta_{RNA{\cdot}Mg} - \Delta\delta_{RNA_i})\left\{\left([Mg^{2+}]_{tot} + [RNA_i]_{tot} + \frac{1}{K_{A_i}}\right) - \left(\left([Mg^{2+}]_{tot} + [RNA_i]_{tot} + \frac{1}{K_{A_i}}\right)^2 - 4[Mg^{2+}]_{tot}[RNA_i]_{tot}\right)^{1/2}\right\}/2[RNA_i]_{tot} \tag{4}$$

where $\Delta\delta_{obs}$ equals the observed chemical shift, $\Delta\delta_{RNA}$ equals that of the unbound (free), and $\Delta\delta_{RNA_i{\cdot}Mg}$ equals that of the fully bound species.

From eqs 1−3 follow eqs 5 and 6:

$$K_{A_i} = \frac{[RNA_i{\cdot}Mg^{2+}]}{([Mg^{2+}]_{tot} - [RNA_i{\cdot}Mg^{2+}])([RNA_i]_{tot} - [RNA_i{\cdot}Mg^{2+}])} \tag{5}$$

$$K_{A_i}([Mg^{2+}]_{tot}[RNA_i]_{tot} - [Mg^{2+}]_{tot}[RNA_i{\cdot}Mg^{2+}] - [RNA_i]_{tot}[RNA_i{\cdot}Mg^{2+}] + [RNA_i{\cdot}Mg^{2+}]^2) = [RNA_i{\cdot}Mg^{2+}] \tag{6}$$

This equation is of second order for $[RNA_i{\cdot}Mg^{2+}]$ and can be rewritten as

$$K_{A_i}[RNA{\cdot}Mg^{2+}]_i^2 - [RNA_i{\cdot}Mg^{2+}](K_{A_i}[Mg^{2+}]_{tot} + K_{A_i}[RNA_i]_{tot} + 1) + K_{A_i}[Mg^{2+}]_{tot}[RNA_i]_{tot} = 0 \tag{7}$$

Thus, two solutions are possible, of which only one yields a physically meaningful value, i.e., a positive concentration for $[RNA_i{\cdot}Mg^{2+}]$, which corresponds to the amount of Mg^{2+} bound at each site "*i*" $[Mg^{2+}]_{bound,i}$

$$[RNA_i{\cdot}Mg^{2+}] = [Mg^{2+}]_{bound,i} = \{(K_{A_i}[Mg^{2+}]_{tot} + K_{A_i}[RNA_i]_{tot} + 1) - ((-(K_{A_i}[Mg^{2+}]_{tot} + K_{A_i}[RNA_i]_{tot} + 1))^2 - 4K_{A_i}^2[Mg^{2+}]_{tot}[RNA_i]_{tot})^{1/2}\}/2K_{A_i} \tag{8}$$

The actual Mg^{2+} concentration available for each of the five binding sites "*i*" $[Mg^{2+}]_{avail,i}$ is thus given by

$$[Mg^{2+}]_{avail,i} = [Mg^{2+}]_{tot} - \sum[Mg^{2+}]_{bound,tot} + [Mg^{2+}]_{bound,i} \tag{9}$$

$[Mg^{2+}]_{avail.i}$ was then plotted versus the chemical shift values of the protons present at or close to this particular binding site (see, e.g., Figure 4), to yield a second set of $K_{A,est2}$ values for each evaluated proton. Again, these second $K_{A,est2}$ estimates were averaged for each of the five individual binding sites to give a higher and more accurate $K_{A,av2}$ value for each site (Table 2). On the basis of these new $K_{A,av2}$ values, the amount of bound Mg^{2+} ions to each binding site was again calculated, and the described procedure was repeated. After five rounds of this iterative approximation procedure, the $K_{A,av}$ values for each binding site did not change any more within their error limits. At this point, the $K_{A,av}$ values of each site were plotted versus the corresponding iteration round and fit to an asymptotic curve fit, leading to the final affinity constant $K_{A,final}$ for each binding site (see also Results and Discussion, Figure 5, and Supporting Information Figure S1).

(27) Sigel, R. K. O.; Sashital, D. G.; Abramovitz, D. L.; Palmer, A. G., III; Butcher, S. E.; Pyle, A. M. *Nat. Struct. Mol. Biol.* **2004**, *11*, 187−192.
(28) Sigel, R. K. O.; Freisinger, E.; Lippert, B. *J. Biol. Inorg. Chem.* **2000**, *5*, 287−299.

In the case of Mg^{2+} coordination to the 5′-terminal di- or triphosphate group, competition with proton binding is taking place at pD 6.7; thus, apparent affinity constants $K^{app}_{A,DP/TP}$ are obtained. These constants can be transformed to pH-independent local stability constants $K_{A,DP/TP}$ by using eq 11 as described in the Results and Discussion section.[29]

Results and Discussion

Localization of Metal Ion Binding Sites in D6-27. Recently, we have identified the metal ion binding sites within the branch-point D6 of the yeast mitochondrial group II intron Sc.ai5γ by using a detailed chemical shift mapping analysis (Figures 1b and 2a).[7] By recording [^{1}H,^{1}H]-NOESY spectra in D_2O we monitored the effect of increasing amounts of Mg^{2+} on the chemical shifts of H2, H8, H5, H6, and H1′ within the D6-27 construct. This allowed us to look at both the nucleobase and the sugar residues, which are located in proximity to potential binding sites like the phosphate groups, the purine N7 positions, or carbonyl oxygens. The addition of $MgCl_2$ affected the protons of residues around the branch point most strongly, with A20 H2 showing the largest change in chemical shift of >0.25 ppm (Figure 2A).[7] In addition, strong influences of Mg^{2+} were observed at the helix end and around the tetraloop, indicative of Mg^{2+} binding in these regions.

Chemical shift mapping does not yield enough information to exactly determine the coordinating atoms to the Mg^{2+} ions, because the chemical shift changes can be caused by either direct metal ion binding or by structural changes due to Mg^{2+} coordination nearby. More precise information could be gained by the line broadening induced by Mg^{2+} on the proton chemical shifts near a coordinating ligand. This effect is caused by an exchange of the coordinating Mg^{2+} ion between a RNA-bound and a RNA-free state, which takes place in an intermediate range on the NMR time scale[30,31] and only affects the electronic environment of protons close to the coordinating atom. Taken together with the chemical shift data, four to five putative binding sites were identified (see Supporting Figure S2): the 5′-phosphate groups at the helix end, the tandem GC base pairs flanking the branch region in helix 1 (H1), the branch (BR) site itself, and one or two metal ion binding sites in the tetraloop (TL) region and the base pairs right below in helix 2 (H2).

In D6-27, the construct that was used in this study, we observed two sets of NOE peaks for the 5′-terminal G1 in a 1:2 ratio, the one with lower intensity belonging to molecules with a triphosphate (TP) residue and the second set to the ones with a diphosphate (DP) moiety. The existence of the diphosphate group was proven by electrospray ionization tandem MS (ESI-MS) (see Supporting Figure S3) and presumably stems from metal ion-assisted partial hydrolysis of the terminal NTP[32,33] during transcription, as neither the GTP stock solution showed any hydrolysis product nor did the ratio of the NOE sets change anymore once the NMR sample was prepared.

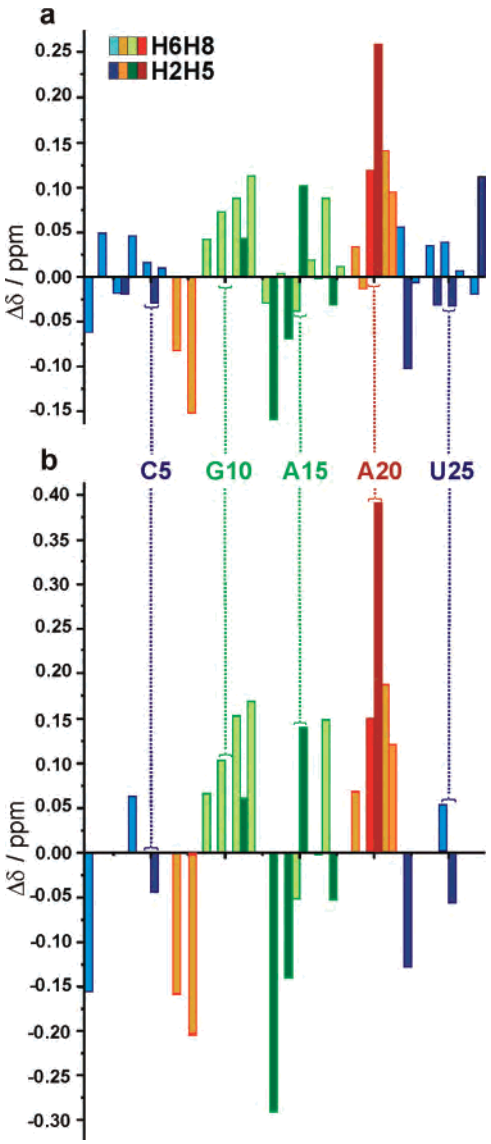

Figure 2. Chemical shift changes within D6-27 upon the addition of Mg^{2+}: (a) Differences in chemical shifts $\Delta\delta$ for the aromatic H6 and H8 protons (light colors) as well as H2 and H5 (dark colors) comparing the Mg^{2+}-free system and the one made upon the addition of 12 mM Mg^{2+}. (b) Difference between the chemical shifts of the Mg^{2+}-free D6-27 and the calculated shifts of the bound species ($\Delta\delta_{RNA\cdot Mg}$, eq 4) for the same protons as in panel (a) after five iterations. It is obvious from the two panels that the chemical shift pattern does not change with the iteration procedure. Panel (a) is adapted from ref 7.

To further validate the assigned metal ion binding regions we performed Mn^{2+} line-broadening experiments, observing imino as well as nonexchangeable protons. The paramagnetic divalent Mn^{2+} ion has extensively been used as a qualitative probe for direct metal ion coordination to RNA, as the line width of signals of nearby protons are significantly broadened upon Mn^{2+} binding.[34−36] [^{1}H]-NMR spectra in 90% H_2O/10% D_2O showed that G1H1 broadens out selectively at 30

(29) It should be noted that all determined affinity constants are "apparent" (or "conditional"), as they are determined at a background of 100 mM KCL (I = 0.1 M).
(30) Pecoraro, V. L.; Hermes, J. D.; Cleland, W. W. *Biochemistry* **1984**, *23*, 5262−5271.
(31) Davis, J. H.; Tonelli, M.; Scott, L. G.; Jaeger, L.; Williamson, J. R.; Butcher, S. E. *J. Mol. Biol.* **2005**, *351*, 371−382.
(32) Sigel, H. *Coord. Chem. Rev.* **1990**, *100*, 453−539.
(33) Sigel, H. *Pure Appl. Chem.* **1998**, *70*, 969−976.

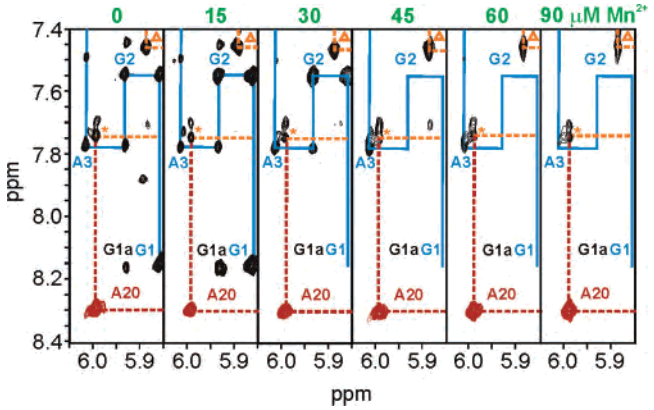

Figure 3. [^{1}H,^{1}H]-NOESY stripes of D6-27 showing the effect of increasing concentrations of Mn^{2+} on resonances assigned to the 5′-end and the branch A20. Intranucleotide H1′−H8 cross-peaks are assigned with the corresponding nucleotide, e.g., G1. Both 5′-termini, i.e., with either a diphosphate (G1) or a triphosphate (G1a) group are indicated. The sequential walk at the 5′-end (solid line) and around A20 (broken line) is indicated in every panel. All peaks at the 5′-end broaden out with the subsequent addition of $MnCl_2$. On the other hand, the branch-point A20H1′−H8 cross-peak is almost not affected, whereas the cross-peaks assigned to the sequential A20H1′−U21H6 (*) and the nearby G7H8−G8H1′ (Δ) become distinctly broader at higher Mn^{2+} concentrations. $MnCl_2$ concentrations are indicated at the top.

μM $MnCl_2$. All other imino resonances of D6-27 broaden out in parallel upon the addition of more Mn^{2+}.

As imino protons of nucleotides are quite far away from potential coordinating atoms, we recorded [^{1}H,^{1}H]-NOESY spectra in D_2O to obtain more accurate information. Again, the H1′−H8 cross-peaks of the 5′-terminal G1 are broadened beyond detection in the presence of 30 μM Mn^{2+}, confirming the strongest binding site at the 5′-terminal end (Figure 3). The intraresidual cross-peak A3H1′−H8 also disappears above 30 μM Mn^{2+}, whereas its H1′−H2 cross-peak only becomes broad at 60 μM. On the 3′-helix end, the intraresidual H1′−H6 of U25, C26, and C27 become broadened at a Mn^{2+} concentration of around 60 μM. The sequential cross-peak between G6H1′ and G7H8 shows a line-broadening effect at around 60 μM Mn^{2+}, as do the cross-peaks involving G10, U11, and G12. This can be taken as a strong indication, indeed, that the tandem GC base pair in helix 1 and the two base pairs right below the tetraloop in helix 2 bind one metal ion each.

The sequential A15H1′−A16H8 peak shows an effect at Mn^{2+} concentrations as low as 30 μM, confirming metal ion binding in the tetraloop. Interestingly, the intraresidual A15H1′−H8 does not get broadened, nor does A15H1′−H2. A16 was not evaluated, as it is lying in the midst of the highly overlapped region below 4.7 ppm.

A very interesting case is presented by the branch region: The cross-peaks associated with the GU wobble pairs flanking the branch A20, like the intraresidual H1′−H8 cross-peaks of G7, G8, and G9, get distinctly broader between 60 and 90 μM. In contrast, A20s intranucleotide H1′−H8 and H1′−H2 as well as the peaks of the internucleotide A20H2−G8H1′ cross-peak are hardly affected (Figure 3), thus indicating that the flanking GU wobble pairs and not A20N7 are involved in M^{2+} binding.

Generally, the H5−H6 cross-peaks are not affected much by Mn^{2+} addition. U11H5/H6 broadens at 60 μM, and C24, U25, and C26 broaden at between 60 and 90 μM. For all other H5−H6 correlations, either no broadening was detected or no evaluation was possible due to severe overlap. Finally, most peaks are affected at higher Mn^{2+} concentration (~120 μM). Thus, the qualitative evaluation of our Mn^{2+} line-broadening studies confirms strongest metal ion coordination to the 5′-end as well as the coordination of similar strengths to helix 1, helix 2, the tetraloop, and the branch region. Furthermore, the Mn^{2+} line broadening suggests the coordination of a metal to the flanking GU wobbles of the branch point but not to the branch adenosine itself.

Taken together, the Mg^{2+} and Mn^{2+} line-broadening data confirm the five metal ion binding sites proposed on the basis of the chemical shift titration data (Figures 1b and 2a). Binding to the phosphate groups at the 5′-terminus is undisputable and should in principle also be the strongest site in the RNA molecule due to the larger negative charge present. Mg^{2+} binding to (tandem) GC base pairs as found in helix 1 and to some extent also in helix 2 is also not surprising and has been observed before: The carbonyl oxygens and N7 positions of the two guanine moieties provide good coordinating sites for metal ions.[37−39] Further Mg^{2+} coordination is observed in the tetraloop region, which is a known Mg^{2+} binding site,[27,31,36,40,41] and, indeed, a recent NMR structure, spin-labeling experiments,[42,43] as well as single-molecule fluorescence measurement[44] in solution indicate that (besides K^+)[45] Mg^{2+} is also required for successful docking of a GNRA tetraloop into its receptor.[31,36] Downey et al.[44] actually showed that only one single Mg^{2+} is needed, which however can also be substituted with two monovalent ions, but of which about 250-fold higher concentrations are needed.

Estimating the Binding Constants of Mg^{2+} to the Five Binding Sites within D6-27. In the hierarchical folding pathway of group II introns, D6 binds last to the active three-dimensional structure by being dragged into the catalytic core by its covalent linkage to D5.[11,12] To overcome the electrostatic repulsion of the tertiary contact formation between these two parts of the ribozyme, a high metal ion content of the free D6 makes sense. In order to understand the docking

(34) Butcher, S. E.; Allain, F. H.-T.; Feigon, J. *Biochemistry* **2000**, *39*, 2174−2182.
(35) Allain, F. H.-T.; Varani, G. *Nucleic Acids Res.* **1995**, *23*, 341−350.
(36) Davis, J. H.; Foster, T. R.; Tonelli, M.; Butcher, S. E. *RNA* **2007**, *13*, 76−86.
(37) Sigel, R. K. O.; Sigel, H. *Met. Ions Life Sci.* **2007**, *2*, 109−180.
(38) Freisinger, E.; Sigel, R. K. O. *Coord. Chem. Rev.* **2007**, *251*, 1834−1851.
(39) Sigel, R. K. O.; Pyle, A. M. *Chem. Rev.* **2007**, *107*, 97−113.
(40) Heus, H. A.; Pardi, A. *Science* **1991**, *253*, 191−194.
(41) Rüdisser, S.; Tinoco, I., Jr. *J. Mol. Biol.* **2000**, *295*, 1211−1223.
(42) Qin, P. Z.; Butcher, S. E.; Feigon, J.; Hubbell, W. L. *Biochemistry* **2001**, *40*, 6929−6936.
(43) Qin, P. Z.; Feigon, J.; Hubbell, W. L. *J. Mol. Biol.* **2005**, *351*, 1−8.
(44) Downey, C. D.; Fiore, J. L.; Stoddard, C. D.; Hodak, J. H.; Nesbitt, D. J.; Pardi, A. *Biochemistry* **2006**, *45*, 3664−3673.
(45) Basu, S.; Rambo, R. P.; Strauss-Soukup, J.; Cate, J. H.; Ferre-D'Amare, A. R.; Strobel, S. A.; Doudna, J. A. *Nat. Struct. Biol.* **1998**, *5*, 986−992.

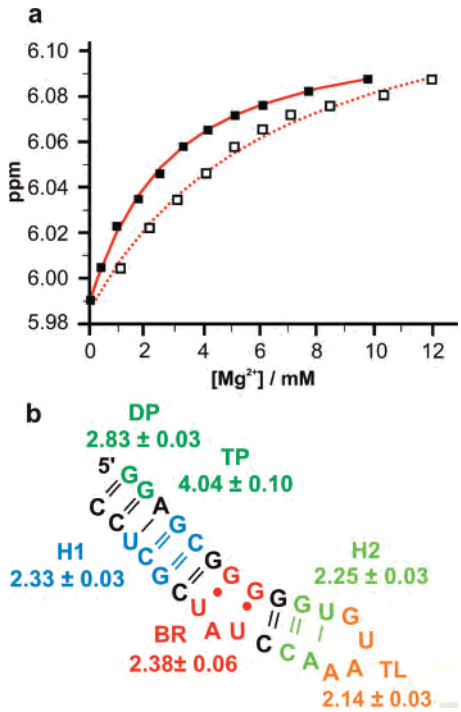

Figure 4. Metal ion binding to D6-27. (a) Plot of the chemical shift change of A20H1′ upon the addition of Mg^{2+} based on eq 4. The chemical shift changes are plotted versus the total Mg^{2+} concentration $[Mg^{2+}]_{tot}$ (□) as well as versus the actually available concentration as calculated after five rounds of iteration (■). A significant improvement of the fit can be seen from the application of the iterative procedure. (b) Secondary structure of D6-27, with the five identified Mg^{2+} binding sites indicated by different colors (see also Table 2 and the Supporting Information Table S1). The given log K_A values correspond to the actual affinity constants at pD 6.7 at each site. The strongest metal ion coordination is found at the 5′-end, indicated in green, with log K_A values for the DP and TP groups, respectively. Further Mg^{2+} binding sites are in H1 (blue), the BR site (red), below the tetraloop in H2 (light green), and the TL itself (orange).

of D6 to the rest of the intron, it will be necessary to know the individual affinities of the five binding sites toward Mg^{2+} ions.

We have therefore performed Mg^{2+} titration experiments recording the change in chemical shift of all aromatic as well as H1′-protons within D6-27. Assuming a non-cooperative binding of Mg^{2+} to each site, eq 1a (see Experimental Section) together with the 1:1 binding isotherm (eq 4)[28,46] holds for every binding pocket. Out of 71 evaluated protons, 41 were fitted to eq 4, and the remaining 30 showed practically no change in chemical shift or could not be traced over all spectra due to severe overlap or line broadening. Fit of the data for each individual proton with eq 4 yielded a first estimate of individual affinities log $K_{A,est}$ between 1.42 ± 0.26 (1σ) and 3.15 ± 0.11 (1σ) (at pD 6.7) (Table 1 and Figure 4a). At first sight, the determined affinities appear to be spread out more or less evenly along D6-27. However, closer examination of the values reveals five regions, where the individual values of log $K_{A,est}$ cluster together within their error limits (Table 1 and Supporting Information Table S1): The first binding region is located at the 5′-end (TP/DP), a second and third one encompass the two base pairs right below the tetraloop (H2), as well as the tetraloop (TL) nucleotides themselves, and a fourth one is found in the branch region (BR). A fifth region of coinciding log $K_{A,est}$ values is located at the tandem G4-C24 and C5-G23 base pairs in the lower stem (H1) (Table 1 and Figures 1b and 4b). These five binding sites assigned on the basis of similar log $K_{A,est}$ values correspond perfectly to the ones defined by qualitatively evaluating the line broadening of the proton resonances observed upon Mg^{2+} binding[7] as well as the above-described studies with Mn^{2+}.

By calculating the weighted mean of the log $K_{A,est}$ values for each binding region, we obtained average log $K_{A,av}$ values for each of the five sites (Table 1 as well as Supporting Information Table S1). The affinity constants obtained for the 5′-end are largest within this RNA with log $K_{A,av1,TP}$ = 3.15 ± 0.11 for the TP end and log $K_{A,av1,DP}$ = 2.35 ± 0.04 for the DP end (Table 2). The relatively high affinity of Mg^{2+} to the 5′-end is expected as the terminal phosphate groups accumulate the highest negative charge density within transcribed RNA. The binding site in helix 1 (H1) around nucleotides G4, C5, G23, C24, and U25 shows a log $K_{A,av1,H1}$ = 1.91 ± 0.09. A very close affinity is observed at the branch region (BR) with log $K_{A,av1,Br}$ = 1.88 ± 0.10. There is a striking consistency in the individual log $K_{A,est}$ values determined from $\Delta\delta$ of the protons at A20 and the neighboring GU wobble pairs: The good agreement of the individual log K_A values for these five nucleotides is a strong indication that as proposed,[7] indeed only a single Mg^{2+} binds in this region. Considering that A20H2 shows by far the largest change in chemical shift, this nicely illustrates that the amount of chemical shift change does not need to coincide with the strengths of a binding site. At G10, U11, A16, and C17 below the tetraloop in helix 2 (H2) the first estimate gives an affinity of log $K_{A,av1,H2}$ = 1.80 ± 0.14, whereas the value for the tetraloop (TL) binding site (G12, U13, A14, and A15) results in log $K_{A,av1,TL}$ = 1.76 ± 0.09. These two mean values for log $K_{A,av1}$ in the tetraloop and the nucleotides right below in helix 2 are very similar and might be assigned to only one binding site. However, the evaluated protons span a distance of 13−14 Å, which is too far for only a single binding site, and we thus propose a simultaneous coordination of two Mg^{2+} ions at this site. Such a scenario has previously been proposed based on fluorescence studies on a related system[47] and is well supported by our accumulated data. With the exception of the 5′-terminal triphosphate group, the determined affinity constants for binding of Mg^{2+} to D6-27 are quite close to each other, meaning that the binding pockets are simultaneously filled with metal ions.

Refinement of Mg^{2+} Affinity Constants for the Five Specified Sites. The simultaneous occupation of the five binding sites within D6-27 has a direct consequence for the calculation of affinity constants. As described above, we have used the *total* Mg^{2+} concentration present in the sample at each step of the titration, as is usually done in such experiments. However, all five binding sites present in D6-27 compete for the free Mg^{2+} ions in solution and become loaded sooner or later according to their individual affinities

(46) Mitchell, P. R. *J. Chem. Soc., Dalton Trans.* **1979**, 771−776.

(47) Menger, M.; Eckstein, F.; Porschke, D. *Biochemistry* **2000**, *39*, 4500−4507.

Table 3. Percentages of Mg^{2+} Available and Bound to Each of the Binding Sites Identified in D6-27 After the First (1st rd) and the Fifth Iteration Round (5th rd). The First Number of Each Entry Represents the Percentage of the Total Mg^{2+} Concentration Bound to One of the Specific Sites, and the Numbers in Parentheses Represent the Corresponding Loading Factor of This Site in Percentage[a,b]

$[Mg^{2+}]_{tot}$		1mM	2 mM	4 mM	5 mM	7 mM	8 mM	10 mM	12 mM
DP	1st rd	9.6 (16.7)	8.3 (29.0)	6.5 (45.4)	5.8 (51.1)	4.9 (59.7)	4.5 (62.9)	3.9 (68.1)	3.4 (72.0)
	5th rd	18.7 (32.8)	14.5 (50.7)	9.8 (68.5)	8.4 (73.4)	6.5 (79.7)	5.8 (81.9)	4.9 (85.1)	4.2 (87.4)
TP	1st rd	15.2 (54.4)	10.0 (71.7)	5.9 (84.1)	4.9 (87.0)	3.6 (90.5)	3.2 (91.6)	2.6 (93.2)	2.2 (94.3)
	5th rd	22.2 (79.2)	12.5 (89.5)	6.6 (94.8)	5.4 (95.6)	3.9 (97.0)	3.4 (97.4)	2.7 (97.9)	2.3 (98.3)
H1	1st rd	6.0 (7.1)	5.6 (13.3)	5.0 (23.5)	4.7 (27.8)	4.3 (35.2)	4.1 (38.3)	3.7 (43.8)	3.4 (48.4)
	5th rd	12.9 (15.1)	11.3 (26.6)	9.0 (42.6)	8.2 (48.4)	6.9 (57.1)	6.4 (60.5)	5.6 (65.9)	5.0 (70.0)
BR	1st rd	5.8 (6.7)	5.4 (12.6)	4.8 (22.5)	4.5 (26.7)	4.1 (33.8)	3.9 (36.9)	3.6 (42.3)	3.3 (46.9)
	5th rd	13.4 (15.8)	11.8 (26.7)	9.4 (44.0)	8.5 (49.8)	7.1 (58.5)	6.6 (61.8)	5.7 (67.1)	5.0 (71.2)
H2	1st rd	4.8 (5.7)	4.6 (10.8)	4.1 (19.6)	4.0 (23.4)	3.6 (30.0)	3.5 (32.9)	3.2 (38.1)	3.0 (42.5)
	5th rd	11.4 (13.4)	10.1 (23.8)	8.3 (38.9)	7.6 (44.6)	6.4 (53.2)	6.0 (56.7)	5.3 (62.2)	4.7 (66.5)
TL	1st rd	4.4 (5.2)	4.2 (9.8)	3.8 (18.0)	3.7 (21.5)	3.4 (27.8)	3.3 (30.6)	3.1 (35.6)	2.8 (39.9)
	5th rd	9.4 (11.0)	8.5 (20.0)	7.1 (33.7)	6.6 (38.9)	5.8 (47.4)	5.4 (50.8)	4.8 (56.5)	4.3 (61.1)
$[Mg^{2+}]_{free}$	1st rd	54.3	61.9	69.9	72.4	76.1	77.6	79.9	81.8
	5th rd	12.1	31.3	49.8	55.3	63.4	66.4	71.0	74.5

[a] The total RNA concentration is 0.85 mM (0.57 mM for DP and 0.28 mM for TP, respectively). [b] In the two bottom rows is given the amount (percentage) of Mg^{2+} still free in solution as calculated with respect to the total concentration of Mg^{2+}.

Table 4. Affinity Constants log $K_{A,est5}$ for Mg^{2+} Binding to D6-27 after the Fifth Iteration Round (see Also Table 1 and Supporting Information Table S1).[a] The Nucleotides Belonging to the Five Individual Binding Sites Are Shaded by Alternative Gray Scales (from left to right: 5′-end (DP/TP); helix 1 (H1); branch region (BR); helix 2 (H2); tetraloop (TL)

	DP/TP			H1			BR				H2		TL	
residue	G1	G2	A3	G4	C5	G6	G7		G8	G9	G10	U11	G12	U13
H1′	2.82 ± 0.16[b]	2.73 ± 0.19[b]	2.24 ± 0.08	n.d.[c]	n.d.[c]	n.d.[c]	2.16 ± 0.04		n.d.[c]	n.d.[c]	n.d.[c]	2.17 ± 0.09	n.d.[d]	2.19 ± 0.09
H2/H5	–	–	n.d.[c]	–	2.29 ±0.15	–	–		–	–	–	2.47 ± 0.08	–	2.11 ± 0.03
H6/H8	n.d.[b,c]	n.d.[b]	n.d.[c]	2.64 ± 0.14	n.d.[c]	n.d.[c]	2.09 ± 0.06		2.48 ± 0.02	2.47 ± 0.16	2.48 ± 0.07	2.18 ± 0.08	2.37 ± 0.18	n.d.[c]
residue	C27	C26	U25	C24	G23	C22	U21	A20	U19	C18	C17	A16	A15	A14
H1′	2.36 ± 0.10	n.d.[c]	1.99 ± 0.26	2.31 ±.08	2.36 ± 0.10	2.27 ± 0.10	2.43 ± 0.15	2..65 ± 0.04	2.42 ± 0.15	n.d.[c]	2.85 ± 0.17	n.d.[c]	2.25 ± 0.09	2.32 ± 0.10
H2/H5	n.d.[c]	n.d.[c]	2.26 ± 0.16	n.d.[c]	–	2.61 ± 0.11	2.63 ± 0.04	2.39 ± 0.09	n.d.[c]	n.d.[c]	2.27 ± 0.11	n.d.[c]	2.49 ± 0.06	2.02 ± 0.08
H6/H8	n.d.[c]	n.d.[c]	2.55 ± 0.15	n.d.[d]	n.d.[c]	n.d.[c]	2.52 ± 0.04	2.67 ± 0.05	2.08 ± 0.09	n.d.[c]	2.20 ± 0.04	n.d.[d]	2.38 ± 0.15	n.d.[c]

[a] The chemical shift changes were obtained from [^{1}H,^{1}H]-NOESY spectra in D_2O (0.85 mM D6-27 RNA, pD 6.7, 100 mM KCl, 10 μM EDTA, 30 °C). The log K_A values were calculated with a Levenberg−Marquardt nonlinear least-squares regression for a single binding isotherm (eq 4), fitted to plots of the chemical shift against the Mg^{2+} concentration available for a certain binding site. The five individual binding sites were identified by Mg^{2+} titrations as well as by Mg^{2+} and Mn^{2+} line-broadening data. All error limits given correspond to 1 standard deviation (1σ). [b] Values are given for Mg^{2+} binding to D6-27 with a 5′-terminal diphosphate. With a 5′-terminal triphosphate group, log K_A = 3.69 ± 0.11 ($G1_{TP}H8$). [c] n.d., not determined, because chemical shift changes were too small. [d] n.d., not determined. as peaks are getting too broad with higher Mg^{2+} concentrations.

(Table 3). As a consequence, the amount of Mg^{2+}available for each of the sites is smaller than the total concentration by the amount bound to the other four sites. For example, whereas the 5′-triphosphate group is already occupied to more than 50% in the Mg^{2+} coordinated form (at 1 mM total Mg^{2+}), the four other sites located within the D6-27 helix are all occupied to less than 8% each (Table 3). However, the freely available Mg^{2+} concentration in solution is only about half of the total concentration present. To correct for this obvious inaccuracy and to obtain more valid affinity constants for each binding site, the following iteration procedure was developed (see also Experimental Section): By using the average affinity constants log $K_{A,av1}$ determined in the previous section, the amount of Mg^{2+} bound to each site at every point of the titration was determined according to eq 8 (Table 3). The amount of Mg^{2+} available for binding to a specific site "*i*" is thus given by the Mg^{2+} coordinated to this site, plus the free concentration of Mg^{2+}, as described by eq 9. These corrected Mg^{2+} concentrations for each site were then used to re-plot the chemical shift changes of the proton resonances for each binding site. A subsequent fit to a 1:1 binding isotherm yielded an improved second estimate of the affinity constant log $K_{A,est2}$ derived from the individual proton resonances throughout D6-27. The individual log $K_{A,est2}$ values of a respective binding site were again analogously averaged. Comparison of the obtained log $K_{A,av2}$ values with those of the first round shows an increase for all affinity constants between 0.19 and 0.26 log units (Table 2). Such a general increase for all binding sites is expected as less available Mg^{2+} is associated with each data point.

On the basis of these newly obtained affinity constants of the second round, the amount of bound Mg^{2+} at each binding site "*i*" was again calculated with eq 8, and subsequently, the concentration of metal ion available for binding at each site was determined. These corrected concentrations were then used for a next round yielding new individual log $K_{A,est3}$ values and subsequent improved numbers for log $K_{A,av3}$. With each consecutive round, the averaged log K_A values increased less, i.e., approached a final value, and after five rounds the log K_A values did not change anymore within their error limits (Tables 2 and 4). The plot of $[Mg^{2+}]_{avail,i}$ at a certain binding site versus the chemical shift of a proton at the same site (Figure 4a) illustrates that the fit of the experimental data with eq 4 improves considerably when comparing the original data and the fifth round of iteration. Such an improved fit is observed for all evaluated protons except for

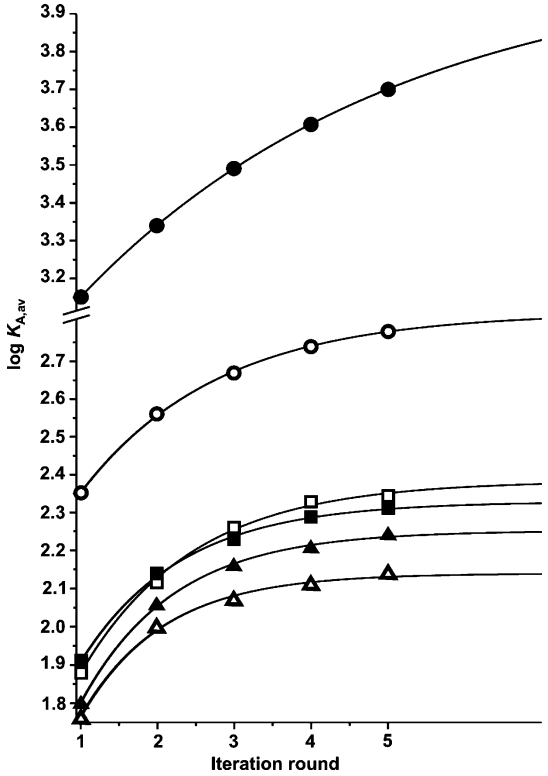

Figure 5. The average log $K_{A,av}$ values of each binding site after each iteration round are plotted versus the iteration number and fitted to an asymptotic function: The triphosphate group at the 5′-end (TP, ●), diphosphate group at the 5′-end (DP, ○), the binding site in H1 (■), the BR site (□), the binding site below the tetraloop in H2 (▲), and the TL itself (Δ).

four cases where the error limits remain the same and two cases (C22H5 and U25H6), where the error limits slightly increase toward the fifth iteration round (Tables 1 and 4). As can be seen by comparing the entries in Tables 1 and 2, the individual log K_A values generally increase by about 0.4−0.5 log units. The largest increase in Mg^{2+} affinity is observed for the 5′-terminal triphosphate group as is reflected by G1H8, where log $K_{A,est}$ value rises from 3.15 ± 0.11 to 3.69 ± 0.11, i.e., by a value of $\Delta\log K_{A,est} = 0.54 \pm 0.16$.

The increased curvature of the fit in round 5 (Figure 4a) reflects the general increase of the log K_A value over the course of the iteration procedure. As the shape of the fitted curve has a direct influence on the chemical shift calculated for the fully bound species Mg·RNA, we plotted the obtained chemical shift changes $\Delta\delta_{RNA\cdot Mg} - \Delta\delta_{RNA}$ after the fifth round (Figure 2b). A comparison with the change in chemical shift upon the addition of 12 mM Mg^{2+} shows that no fundamental change in the pattern occurs, but that the differences between large and small effects are more pronounced.

As mentioned above, with each consecutive iteration round the increase in the log $K_{A,av,i}$ values become smaller, i.e., these values approach a final value. To calculate the final affinity constants log $K_{A,fin}$, we plotted the average log $K_{A,av}$ values of each round versus the number of the iteration and fitted the data to an asymptotic function (Figure 5). The final log $K_{A,fin}$ values are only slightly higher than the log $K_{A,av5}$ values and the same within the error limits for the four internal Mg^{2+} binding sites (Table 2), showing that five rounds already give a very good estimate of the final value. These final values are given in column 7 of Table 2 and vary between $\log K_{A,fin,TP} = 4.04 \pm 0.10$ for the triphosphate and $\log K_{A,fin,TL} = 2.14 \pm 0.03$ for the tetraloop. Hence, an increase of between 0.38 ± 0.09 and 0.89 ± 0.15 log units (Table 2, column 8) in affinity is observed at the individual binding sites when taking into account the amount of Mg^{2+} ion bound to the other sites.

As an internal control for this iterative refinement procedure, we used the log $K_{A,fin}$ values to calculate $[Mg^{2+}]_{free}$ for each binding site by using eqs 1b and 7. If our procedure is consistent within itself, then each binding site must "see" an equal free Mg^{2+} concentration. Indeed, these values correspond very well to each other for every applied Mg^{2+} concentration (Supporting Information Table S2).

Mg^{2+} Binding to the 5′-Terminal Phosphate Groups. As mentioned above, the D6-27 molecules are present in solution with either a terminal triphosphate or a diphosphate group. Mg^{2+} binding to these two groups needs some closer evaluation. Both are excellent binding sites[37,48−52] for Mg^{2+}, as is also illustrated by the final values of $\log K^{app}_{A,TP} = 4.04 \pm 0.10$ and $\log K^{app}_{A,DP} = 2.83 \pm 0.03$. However, it is important to note that the given values are *apparent* constants (as indicated by the superscript "app"), because at a pD level of 6.7, at which the experiments were carried out, a competition between the proton (actually a deuterium cation, D^+) and Mg^{2+} exists for binding at the terminal phosphate residue. Hence, these two values are valid only at the given pD value. This contrasts with all the other binding sites of D6-27 RNA for which no such competition exists because their pK_a values are far below the physiological pH range. Therefore, in all these instances the values listed in Table 2 are the actual stability constants for Mg^{2+} binding at the various sites.

The proton competition at the terminal diphosphate or triphosphate residue, respectively, can be accounted for by considering the corresponding pK_a values of these monoprotonated phosphate groups. These acidity constants are not known for D6-27, but one may safely assume that they are very similar to those of nucleoside 5′-triphosphates ($pK^H_{H(NTP)} = 6.50 \pm 0.05$)[53,54] and nucleoside 5′-diphosphates ($pK^H_{H(NDP)} = 6.40 \pm 0.05$).[51,52] The reason for this similarity is that the nucleosidyl residues are rather far away from the site of deprotonation, i.e., the monoprotonated terminal phosphate group. Indeed, the values for $H(GTP)^{3-}$ ($pK^H_{H(GTP)} = 6.50 \pm 0.02$)[49] and $H(GDP)^{2-}$ ($pK^H_{H(GDP)} = 6.38 \pm 0.01$)[37] fit into the indicated picture. As D6-27 has a 5′-

(48) Scheller, K. H.; Hofstetter, F.; Mitchell, P. R.; Prijs, B.; Sigel, H. *J. Am. Chem. Soc.* **1981**, *103*, 247−260.
(49) Sigel, H.; Bianchi, E. M.; Corfù, N. A.; Kinjo, Y.; Tribolet, R.; Martin, R. B. *Chem.−Eur. J.* **2001**, *7*, 3729−3737.
(50) Sigel, H.; Griesser, R. *Chem. Soc. Rev.* **2005**, *34*, 875−900.
(51) Sajadi, S. A. A.; Song, B.; Gregan, F.; Sigel, H. *Inorg. Chem.* **1999**, *38*, 439−448.
(52) Bianchi, E. M.; Sajadi, S. A. A.; Song, B.; Sigel, H. *Chem.−Eur. J.* **2003**, *9*, 881−892.
(53) Sigel, H.; Bianchi, E. M.; Corfu, N. A.; Kinjo, Y.; Tribolet, R.; Martin, R. B. *J. Chem. Soc., Perkin Trans.* **2001**, *2*, 507−511.
(54) Sigel, H. *Pure Appl. Chem.* **2004**, *76*, 375−388.

G, we shall use these latter values for our evaluation. Application of eq 10

$$pK_{a/D_2O} = 1.015pK_{a/H_2O} + 0.45 \quad (10)$$

provides for D_2O as solvent,[55] $pK^{D}_{D(GTP)} = 7.05$, and $pK^{D}_{D(GDP)} = 6.93$. The competition between the proton and a metal ion is defined by eq 11:[56,57]

$$\log K_{A,DP/TP} = \log K^{app}_{A,DP/TP} + \log\left(1 + \frac{[D^+]}{K_{a/D_2O}}\right) \quad (11)$$

Hence, by applying this equation and inserting the apparent affinity constants (Table 2), the actual local stability constants $\log K_{A,TP} = 4.55 \pm 0.10$ for the triphosphate and $\log K_{A,DP} = 3.26 \pm 0.03$ for the 5′-diphosphate are obtained. The smaller affinity of the diphosphate group by about 1.3 log units compared with the value obtained for the triphosphate end is well in line with the reduced number of binding sites and the lower negative charge at the phosphate residue.

Conclusion

Metal ions are key players in group II intron ribozymes, not only directing the folding process and stabilizing the complicated tertiary structure but also being directly implicated in catalysis.[13,14,17,58] It is evident that any larger RNA oligonucleotide will exhibit several metal ion binding sites due to the manifold negative charges present. However, in terms of the determination of affinity constants of M^{n+} ions to such sites, this fact has commonly been overlooked. Here, we have shown by detailed evaluation of metal ion binding to the branch domain construct D6-27 of the group II intron Sc.ai5γ that the amount of bound metal ions to other sites needs to be accounted for to obtain accurate local affinity constants, often also addressed as microstability constants, for a given site. As a consequence of the simultaneous accounting for the other binding sites present in the RNA, the available Mg^{2+} concentration for binding to a specific site becomes successively smaller with each iteration (Table 3 and Figure 4a). The obtained log K_A values are between about 0.4 and 0.9 log unit larger than the ones obtained without accounting for Mg^{2+} binding to the other sites (Table 2). To the best of our knowledge, this is the first time that the effectively available Mg^{2+} concentration for each binding site within a larger RNA molecule is taken into account for the calculation of the individual affinity constants. The iterative method described here is generally applicable not only to RNAs but to any ligand that binds multiple metal ions.

The final intrinsic affinity constants obtained here by this novel iterative procedure provide a more exact picture of the metal ion binding properties of such a RNA hairpin, although the size of the values is still within the range[27,59] of affinities observed before. However, the more metal ions simultaneously bind to a RNA molecule (or any other ligand) and the higher these affinities are, the more the rest of the intrinsic binding constants are affected, and hence, an iterative calculation as described here is needed. Higher affinities are observed by either applying a different kind of metal ion[38,44] or by looking at systems where the Mg^{2+} ion is directly involded in folding.[44,60] For example, it has been shown that only one Mg^{2+} ion is required for successful docking of a GAAA tetraloop into its receptor, having a log $K_A = 3.06 \pm 0.05$.[44] This value is about 0.9 log unit higher than that of $\log K_{A,fin,TL} = 2.14 \pm 0.03$ but can be explained by the putative additional interaction of the Mg^{2+} ions with the tetraloop receptor, which is not present in our case. At the same time, this comparison suggests that the Mg^{2+} ion is already bound to the GAAA tetraloop before docking and is subsequently more tightly embedded after the tertiary structure formation is completed.

Excluding the 5′-end, the four binding sites within D6-27 all show similar affinities toward Mg^{2+} ions in that no cooperativity was observed. These four Mg^{2+} ions compensate about 30% of the total 27 negatively charged phosphate groups, which is clearly above the 10% commonly observed.[38,39] Hence, four specific binding sites seem surprisingly high for a hairpin of this size. However, recent results showed that D6 does not exhibit strong crucial tertiary contacts to other intronic domains and that the covalent linkage to D5 suffices to guide the binding of D6 into the catalytic core,[8,11,12] where D6 gets into close contact with the coordination loop in D1.[61] In light of these results, a high number of equally strong bound metal ions to D6 will facilitate docking of the branch domain into D1 and D2 simply by compensating for the repulsive negative charges of the individual domains.

The extent of the line-broadening effect of Mn^{2+} on the different regions within D6-27 parallels the affinity constants obtained for Mg^{2+} binding to the five binding sites, illustrating that Mn^{2+} is a reasonably good mimic of Mg^{2+}.[38,39] Titration as well as paramagnetic line-broadening studies show that the strongest binding site in D6-27 for Mg^{2+} and Mn^{2+} is located at the 5′-end of this hairpin, being composed of a diphosphate or a triphosphate chain, respectively. Both groups have a considerably higher affinity toward metal ions than, e.g., the branch region, which can be easily explained by the higher negative charge of the free phosphate groups. The actual affinity constants $\log K_{A,DP} = 3.26 \pm 0.03$ for Mg^{2+} binding to the diphosphate residue and $\log K_{A,TP} = 4.55 \pm 0.10$ for the triphosphate end (Table 2, footnote) are almost identical to the ones previously determined for the $Mg(GDP)^-$ ($\log K^{Mg}_{Mg(GDP)} = 3.39 \pm 0.04$)[37,62] and the

(55) Martin, R. B. *Science* **1963**, *139*, 1198, 1203.
(56) Scheller, K. H.; Abel, T. H. J.; Polanyi, P. E.; Wenk, P. K.; Fischer, B. E.; Sigel, H. *Eur. J. Biochem.* **1980**, *107*, 455−466.
(57) Sigel, H.; McCormick, D. B. *Acc. Chem. Res.* **1970**, *3*, 201−208.
(58) Swisher, J. F.; Su, L. J.; Brenowitz, M.; Anderson, V. E.; Pyle, A. M. *J. Mol. Biol.* **2002**, *315*, 297−310.
(59) Blad, H.; Reiter, N. J.; Abildgaard, F.; Markley, J. L.; Butcher, S. E. *J. Mol. Biol.* **2005**, *353*, 540−555.
(60) Das, R.; Travers, K. J.; Bai, Y.; Herschlag, D. *J. Am. Chem. Soc.* **2005**, *127*, 8272−8273.
(61) Hamill, S.; Pyle, A. M. *Mol. Cell* **2006**, *23*, 831−840.
(62) Bianchi, E. M. *Comparison of the Stabilities and Solution Structures of Metal Ion Complexes Formed with 5′-Di- and 5′-Triphosphates of Purine Nucleotides*; Logos Verlag: Berlin, 2003.

$Mg(GTP)^{2-}$ complexes (log $K^{Mg}_{Mg(GTP)} = 4.31 \pm 0.04$).[49] This accordance nicely demonstrates that results obtained for mononucleotides can be transferred to larger nucleic acids if no further interactions take place.[38]

In both cases, i.e., the terminal di- or triphosphate group, the G1H8−H1′ resonances become very broad with increasing Mg^{2+} concentration (this effect is more pronounced in the case of the diphosphate). This line broadening can be attributed to macrochelate formation of the phosphate-coordinated Mg^{2+}, i.e., to an additional interaction with the N7 position of G1 (possibly also involving O6). Such macrochelates have been shown to occur with a formation degree of about 20% in $Mg(GTP)^{2-}$ and $Mg(GDP)^{-}$ species.[37,49,50,52,62] The indicated formation degree of 20% of the macrochelate corresponds to a stability increase of about 0.1 log unit, whereas stability increases of 0.3 or 0.5 log units correspond to formation degrees of about 50 or 70%, respectively.[38,49,50,63] To the best of our knowledge, this is the first time that affinity constants for Mg^{2+} binding to 5′-terminal phosphate groups of a larger RNA hairpin have been determined. Nevertheless, more experiments are needed to characterize the binding of Mg^{2+} to helix ends of RNAs in more detail and to exactly specify all the coordination sites involved.

Our Mg^{2+} binding studies reveal a further important point: At physiological pH, the affinity of Mg^{2+} toward the oxygen atoms of the terminal phosphate groups is in a first approximation significantly higher than toward any other coordinating atom in a nucleic acid. This is in good agreement with two recent studies on the dinucleotides $pUpU^{3-}$ and $d(pGpG)^{3-}$.[64,65] Terminal mono-, di-, and triphosphate residues are very abundant in living cells, e.g., a human being has a daily ATP-turnover equivalent to the body weight.[66] The here-determined affinities for D6-27 in comparison with the known values for monophosphate monoesters or nucleoside monophosphates (log $K^{Mg}_{Mg(NMP)} = 1.6$)[37,63] illustrate that a RNA site can easily compete for Mg^{2+} ions in the cell. Compared to $Mg(NDP)^{-}$ complexes, the affinities are similar, and hence, RNA still has a good chance in this competition. However, in order to compete for Mg^{2+} with the highly abundant triphosphate groups of ATP, the metal ion binding pockets within RNA need to be perfectly formed by several coordinating atoms, possibly connected with a reduced polarity,[39] thereby adding up small increments to offer a comparable stability.

(63) Sigel, H.; Song, B. *Met. Ions Biol. Syst.* **1996**, *32*, 135−206.
(64) Knobloch, B.; Suliga, D.; Okruszek, A.; Sigel, R. K. O. *Chem.—Eur. J.* **2005**, *11*, 4163−4170.
(65) Knobloch, B.; Sigel, H.; Okruszek, A.; Sigel, R. K. O. *Chem.—Eur. J.* **2007**, *13*, 1804−1814.
(66) Banks, B. E. C. *Chem. Br.* **1996**, *32 (May)*, 28.

Abbreviations

BR, metal ion binding site in the branch region of D6-27; D1, D2, D3, D4, D5, and D6, domains 1, 2, 3, 4, 5, and 6 of the group II intron Sc.ai5γ; D6-27, shortened domain 6 construct used in this study; D56, RNA construct containing domains 5 and 6; DP, 5′-terminal diphosphate group of D6-27; H1, metal ion binding site in helix 1 of D6-27; H2, metal ion binding site in helix 2 of D6-27; Sc.ai5γ, group II intron ribozyme located in the cytochrome oxidase 1 gene of *Saccharomyces cerevisiae*; TL, metal ion binding site at the tetraloop of D6-27; TP, 5′-terminal triphosphate group of D6-27.

Acknowledgment. We thank Maya Furler and Andrea Muntean for the expression and purification of T7 RNA polymerase, Dr. Bernd Knobloch for the preparation of the $MgCl_2$ and $MnCl_2$ stock solutions in D_2O, Dr. Cinzia Finazzo and Jonathan Coles for helpful suggestions regarding the "automatization" of the iterative Mg^{2+} binding procedure as well as Renate Rieder and Prof. Dr. Ronald Micura (University of Innsbruck, Austria) for the recording of the ESI-MS spectra. Financial support by the Swiss National Science Foundation (SNF-Förderungsprofessur to R.K.O.S.) is gratefully acknowledged.

Supporting Information Available: Graphical representation of the changes of the log $K_{A,av}$ values over the course of the iteration; illustration of the line broadening induced by Mg^{2+}; ESI-MS spectrum of D6-27, as well as two tables listing the hydrogen atoms combined to define the individual binding regions and the $[Mg^{2+}]_{free}$ value calculated with the final log $K_{A,fin}$ values of each binding site. This material is available free of charge via the Internet at http://pubs.acs.org.

IC701627T